Applied Physics Letters

Thermally tunable whispering-gallery mode cavities for magneto-optics

Cite as: Appl. Phys. Lett. **116**, 161110 (2020); https://doi.org/10.1063/5.0006367
Submitted: 04 March 2020 . Accepted: 06 April 2020 . Published Online: 22 April 2020

Serge Vincent, Xin Jiang, Philip Russell, and Frank Vollmer

Applied Physics Letters ARTICLE scitation.org/journal/apl

Thermally tunable whispering-gallery mode cavities for magneto-optics

Cite as: Appl. Phys. Lett. **116**, 161110 (2020); doi: 10.1063/5.0006367
Submitted: 4 March 2020 · Accepted: 6 April 2020 ·
Published Online: 22 April 2020

Serge Vincent,[1,a)] Xin Jiang,[2] Philip Russell,[2] and Frank Vollmer[1,b)]

AFFILIATIONS

[1]Living Systems Institute, School of Physics, University of Exeter, Exeter EX4 4QD, United Kingdom
[2]Max Planck Institute for the Science of Light, Staudtstrasse 2, 91058 Erlangen, Germany

[a)]Email: sv316@exeter.ac.uk
[b)]Author to whom correspondence should be addressed: f.vollmer@exeter.ac.uk

ABSTRACT

We report the experimental realization of magneto-optical coupling between whispering-gallery modes in a germanate ($56GeO_2$-31PbO-$9Na_2O$-$4Ga_2O_3$) microspherical cavity due to the Faraday effect. An encapsulated gold conductor heats the resonator and tunes the quasi-transverse electric (TE) and quasi-transverse magnetic (TM) polarized modes with an efficiency of ∼65 fm/V at a peak-to-peak bias voltage of 4 V. The signal parameters for a number of heating regimes are quantified to confirm sensitivity to the generated magnetic field. The quasi-TE and quasi-TM resonance frequencies stably converge near the device's heating rate limit (equivalently, bias voltage limit) in order to minimize inherent geometrical birefringence. This functionality optimizes Faraday rotation and thus enables the observation of subsequent magneto-optics.

Optical devices that exploit whispering-gallery modes (WGMs) have gradually become ubiquitous.[1] The WGM cavity has demonstrated strong optomechanical interactions,[2,3] lased at ultralow thresholds,[4] established parity-time symmetric systems,[5] and detected single atomic ions near plasmonic nanoantennae.[6] Tuning of WGMs outside of irreversible modification[7,8] has been achieved by refractive index modulation, such as from mechanical strain/pressure,[9–12] electro-optics,[13–15] or thermal effects.[16–20] Thermo-optical control is typically realized by selecting a high-thermo-optic coefficient material for the cavity[18,19] or relying on absorption based heating,[16,17] wherein the former involves an integrated heating element. Tuning of glass WGM cavities through an internal metallic conductor, however, can be intractable due to glass crystallization during fabrication. While melting the dielectric at a temperature below the conductor's melting point, nucleation sites develop and with crystal growth inhibit WGM circulation. For sensing applications in a stochastic environment, there is also a need for laser jitter suppression when detecting nanoparticles[21] and the removal of background drift when thermally characterizing polymers.[22]

By way of optomechanics and magnetostriction, on-chip WGM based magnetometers[23] have detected magnetic fields with sensitivities as small as hundreds of $pT/\sqrt{Hz}$.[24] More generally, magneto-optical coupling in a WGM resonator has been studied for transported magnetic fluids[25,26] and for the resonator material itself.[27] Cavity optomagnonics in yttrium iron garnet (YIG) microspheres[28,29] offers coherent magnon-to-photon interconversion at optical and microwave frequencies, justifying the use of magnons as information carriers. An applied magnetic field B modifies the cavity dielectric tensor by first and second order magnetization, respectively, known as the Faraday and Voigt effects.[30] The quasi-transverse electric (TE) and quasi-transverse magnetic (TM) WGM resonance frequencies are split by the cavity boundary conditions, i.e., by a geometrically induced birefringence Δn_g, and are mixed by the Faraday effect.[31] One conclusion that was drawn in Ref. 31 was that Δn_g quenches the overall Faraday rotation. Minimizing Δn_g in turn maximizes the magnetic field sensitivity and so polarization rotation at the output coupler becomes significant. Cavity-enhanced polarimetry[32] is an extension of this operational principle through which chiral measurement can be considered.

In this paper, we present a WGM sensing platform that dually incorporates thermal tuning and magneto-optical responsivity. A germanate ($56GeO_2$-31PbO-$9Na_2O$-$4Ga_2O_3$) microsphere with a high Verdet constant is fabricated with a central gold conducting wire to modulate the WGM resonance via heating and induce a magnetic field on the order of 1 G. The cavity-wire structure is fashioned by inserting a sub-millimeter diameter gold wire into a germanate capillary, then a capillary segment with a wire protrusion is melted inside a ceramic microheater. Convection and surface tension promote the formation of a germanate microspherical profile around the wire (with the cavity radius on the order of hundreds of μm) and glass isotropy is ensured by the germanate's slower crystallization rate. The wire geometry creates a B-field that is parallel or antiparallel to the WGM propagation direction throughout current reversal in time. Critically, as the cavity refractive index (n_c) profile guides quasi-TE and quasi-TM modes differently, we show that Δn_g decreases with thermal conductance throughout the cavity with the increasing root-mean-square amplitude of the oscillating bias voltage. This WGM tunability scheme excludes large and expensive electromagnets in order to limit the device footprint.

Scans were performed across WGM resonances using a tunable external cavity laser of central wavelength $\lambda = 642$ nm in the geometry shown in Fig. 1. Light is focused onto the internal surface of a rutile prism and, through frustrated total internal reflection, couples to the germanate microsphere at 5% efficiency in order to excite WGMs. We note that the prism is birefringent with an ordinary refractive index n_o and an extraordinary refractive index n_e above that of the germanate ($n_c < 2 < n_o < n_e$) within the chosen optical bandwidth. The WGM microsphere in contact with this prism is doubly clamped above a metal-on-insulator biasing chip [Fig. 1(a)] and the enclosed 150-μm diameter gold wire supports actuating currents of up to a few amperes. Spectral characterization of the germanate's Verdet constant [Fig. 1(b)] determined a value of ~ 25 rad/(Tm) near WGM resonances. Nevertheless, initial peak tracking of the resonance line shape in Fig. 1(c) for a triangular bias voltage $V(t)$ suggests dominant thermal influences. In principle, for a local temperature change ΔT, signal rectification arises from Joule heating

$$\Delta\lambda_{Res}(t) \propto \Delta T(t) \propto V^2(t). \quad (1)$$

Linewidth narrowing and broadening follows the heating cycle with a π phase delay with respect to the resonant wavelength λ_{Res}. When the suspended microsphere contacts the prism, forces acting on the sphere-stem cantilever[33] from capacitance at the soft glass interface and flexion from heating can vary the coupling to the WGM and hence alter the linewidth. The magnetic field oscillation frequency f_M is not equal to that of the recorded response of Fig. 1(c)—what is instead observed is a WGM perturbation at $2f_M$ due to heat conduction that is independent of the current direction. The trace's noise floor in the tens of fm range, in this case derived from the cavity quality factor $Q = \lambda_{Res}/\delta\lambda \approx 2 \times 10^5$, exceeds the laser phase noise.

Further investigation of the perturbed WGM resonance was carried out by frequency domain analysis. The entire resonance trace of Fig. 2(a) was decomposed into its frequency components [Fig. 2(b)], revealing the expected DC component and $2f_M$ peaks for a full-wave rectified resonance signal response. These peaks originate from thermal nonlinearities; however, f_M peaks also exist within the spectrum. Normalized spectral peak amplitude vs frequency curves in Fig. 2(b) for the two separate series of peaks differ in bandwidth, thus indicating separate time constants. The model proposed in Ref. 31 derived from the coupled mode theory contextualizes this disparity: once the B-field is sufficient to overcome the geometrical birefringence Δn_g, mode mixing produces deviations in quasi-TE and quasi-TM WGM eigenfrequencies away from degeneracy. Consequently, a partial-wave rectified resonance shift pattern from a weak intracavity Faraday effect would exhibit the f_M peak seen in our experiment. With lower Δn_g, coupling between quasi-TE and quasi-TM WGMs is detected at lower magnetic field thresholds.

Faraday rotation θ_F is optimized in the unquenched regime ($\Delta n_g = 0$) and highly dependent on the magnetic field strength. Calculations in Fig. 3(a) outline that θ_F and hence the shift $\Delta\lambda_{Res}$ for a tellurite WGM microsphere are linear with the B-field. Simulated fundamental quasi-TE and quasi-TM WGMs with azimuthal mode order $m = 975$ (i.e., near the experimental operating wavelength) places the operating points at $\Delta n_g = 0.00146$, neglecting the cavity index profile variation from thermo-refractivity and thermal expansion. Accounting for this tuning, on the other hand, can lead to a displacement in the radial position of the guided WGM intensity maxima. Figure 3(b) depicts the experimental resonance trace when increasing the root-mean-square amplitude of the bias voltage. By fixing the duty cycle of the electrical signal, the time-averaged heating of the

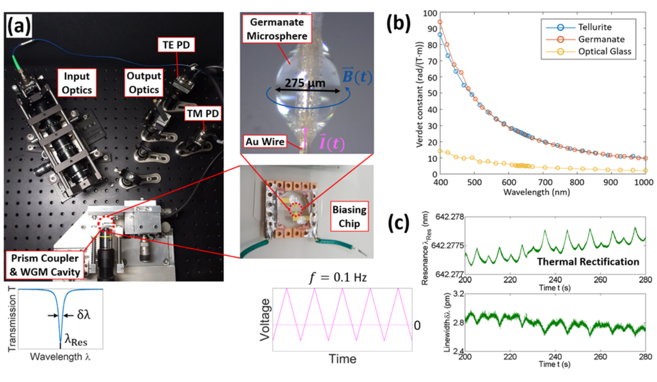

FIG. 1. WGM excitation in a magneto-optical microsphere with a confined conductor. (a) Experimental setup. (b) Measured Verdet constant spectra for optical and soft glasses. (c) Device operation with a triangular wave current input. Heat generated by the electrical conductor results in a WGM resonant wavelength shift proportional to the square of the voltage, such that the resonance oscillation frequency is exactly twice that of the current when there is no DC offset.

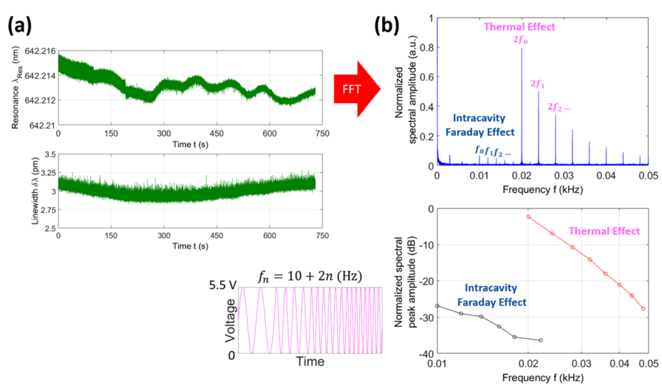

FIG. 2. Fast Fourier transform (FFT) of the WGM resonance response to frequency ramping. (a) Time trace for a sinusoidal current input. The oscillation frequency is increased from 10 to 24 Hz in discrete steps of 2 Hz. (b) Fourier spectrum and semi-log plot of the normalized spectral amplitude vs frequency.

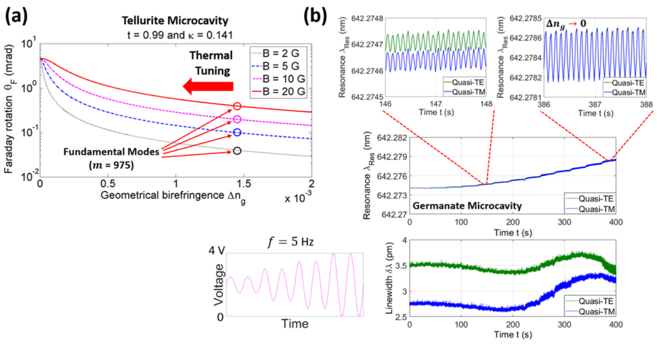

FIG. 3. Thermal tuning of quasi-TE and quasi-TM WGMs to minimize geometrical birefringence. (a) Computed Faraday rotation vs geometrically induced birefringence for a 50-μm radius tellurite microspherical cavity. The transmission coefficient $t = 0.99$ and coupling coefficient $\kappa = 0.141$ match the simulations from Ref. 31. (b) Converging quasi-TE and quasi-TM WGM resonant wavelengths with increasing amplitude of the sinusoidal current input. Note that the resonant wavelength traces are in-phase.

microsphere enforces a radial thermal gradient that equalizes the quasi-TE and quasi-TM WGM eigenfrequencies. These modes begin with different penetration depths into the external dielectric, and with precise thermal feedback, may converge toward minimal geometrical birefringence. At a peak-to-peak bias voltage $V_{pp} = 4$ V, the tuning efficiency reaches ~ 65 fm/V and the modes differ in resonant wavelength by less than 1 pm. The amplitude of in-phase shift $\Delta\lambda_{Res}$ for these modes scales linearly with V_{pp} and the signal undergoes a steeper rise toward the peak, in agreement with thermal and intracavity Faraday effect superposition. WGM resonant linewidths are similar in oscillation and close in value (≤ 0.5 pm at $V_{pp} = 4$ V), remaining synchronous irrespective of the superimposed perturbations.

The findings in this study provide preliminary evidence for the optical WGM resonator analog of polarization rotation in a soft glass cavity. A cost-effective microheater with electrical interfacing was used to tune the WGM resonances and reduce geometrically induced birefringence. The latter enhances the quasi-TE and quasi-TM polarization coupling per round trip in the presence of a proximate magnetic field aligned with mode propagation. Magnetization dynamics could be explored, such as the possibility of lasing by way of magnon Brillouin scattering. Nonreciprocal Brillouin scattering can bring selective creation and annihilation of magnons in the Kittel mode, alongside chiral features embedded in the spin dynamics of a ferromagnetic YIG microcavity.[28,29] Due to the solubility of the germanate glass, any WGM measurement in solution may require the coating of a protective layer [e.g., a perfluoro(1-butenyl vinyl ether) polymer] around the cavity. By satisfying this criterion, we anticipate future chiral sensing of enantiomer layers on the cavity surface. Distinguishing the chirality of and detecting Faraday rotation from single molecules will, however, necessitate greater specificity and signal enhancement. Single-molecule chirality is largely unattainable in cavity polarimetry schemes[30] as the requisite resolution falls below the shot noise. A signal-reversing WGM biosensor based on the intracavity Faraday effect may circumvent this pitfall by isolating for a weak yet local chiral signal. This is afforded by exceptional points[5] and/or mode hybridization through coupling to localized surface plasmons of metallic nanoparticles.[6] Plasmonic nanoantennae from Ref. 6 may be functionalized with organic molecules possessing a substantial Verdet constant {e.g., 1,3,5-trimethyl-2,4,6-tris[2–(4-nitrophenyl)ethynyl]benzene/TTB[34]} as they would be individually detectable and responsive to magnetic field fluctuations in the optoplasmonic system. Another promising avenue is the detection of magnetic field-dependent protein behavior, such as cryptochrome signaling.[35] Spin states correlated with such biochemical reactions could be manipulated with the local magnetic field and probed according to the magneto-optical coupling of the resonator, i.e., through resolvable discrepancies between the quasi-TE and quasi-TM WGM resonance response.

The authors would like to thank Rémy Soucaille for his contribution in characterizing the glasses' Verdet constants. S.V. also thanks Peter Rakitzis and Matthew Foreman for their valuable discussions. Resonance peaks in the measured spectra were tracked and analyzed using software developed by Martin Baaske. This work was supported by a H2020 FET Open grant (ULTRACHIRAL, No. 737071) issued by the European Research Council.

REFERENCES

1. K. J. Vahala, "Optical microcavities," Nature **424**, 839–846 (2003).
2. H. Rokhsari, T. J. Kippenberg, T. Carmon, and K. J. Vahala, "Radiation-pressure-driven micro-mechanical oscillator," Opt. Express **13**, 5293–5301 (2005).
3. T. J. Kippenberg, H. Rokhsari, T. Carmon, A. Scherer, and K. J. Vahala, "Analysis of radiation-pressure induced mechanical oscillation of an optical microcavity," Phys. Rev. Lett. **95**, 033901 (2005).
4. S. M. Spillane, T. J. Kippenberg, and K. J. Vahala, "Ultralow-threshold Raman laser using a spherical dielectric microcavity," Nature **415**, 621–623 (2002).
5. B. Peng, Ş. K. Özdemir, F. Lei, F. Monifi, M. Gianfreda, G. L. Long, S. Fan, F. Nori, C. M. Bender, and L. Yang, "Parity-time-symmetric whispering-gallery microcavities," Nat. Phys. **10**, 394–398 (2014).
6. M. D. Baaske and F. Vollmer, "Optical observation of single atomic ions interacting with plasmonic nanorods in aqueous solution," Nat. Photonics **10**, 733–739 (2016).
7. L. Ma, S. Kiravittaya, V. A. B. Quiñones, S. Li, Y. Mei, and O. G. Schmidt, "Tuning of optical resonances in asymmetric microtube cavities," Opt. Lett. **36**, 3840–3842 (2011).
8. E. Gil-Santos, C. Baker, A. Lemaître, S. Ducci, C. Gomez, G. Leo, and I. Favero, "Scalable high-precision tuning of photonic resonators by resonant cavity-enhanced photoelectrochemical etching," Nat. Commun. **8**, 14267 (2017).
9. W. von Klitzing, R. Long, V. S. Ilchenko, J. Hare, and V. Lefèvre-Seguin, "Frequency tuning of the whispering-gallery modes of silica microspheres for cavity quantum electrodynamics and spectroscopy," Opt. Lett. **26**, 166–168 (2001).
10. J. P. Rezac and A. T. Rosenberger, "Locking a microsphere whispering-gallery mode to a laser," Opt. Express **8**, 605–610 (2001).
11. T. Ioppolo and M. V. Ötügen, "Pressure tuning of whispering gallery mode resonators," J. Opt. Soc. Am. B **24**, 2721–2726 (2007).
12. M. Pöllinger, D. O'Shea, F. Warken, and A. Rauschenbeutel, "Ultrahigh-Q tunable whispering-gallery-mode microresonator," Phys. Rev. Lett. **103**, 053901 (2009).
13. P. Rabiei, W. H. Steier, C. Zhang, and L. R. Dalton, "Polymer micro-ring filters and modulators," J. Lightwave Technol. **20**, 1968–1975 (2002).
14. A. A. Savchenkov, V. S. Ilchenko, A. B. Matsko, and L. Maleki, "Tunable filter based on whispering gallery modes," Electron. Lett. **39**, 389–391 (2003).
15. Z. Fang, S. Haque, J. Lin, R. Wu, J. Zhang, M. Wang, J. Zhou, M. Rafa, T. Lu, and Y. Cheng, "Real-time electrical tuning of an optical spring on a monolithically integrated ultrahigh Q lithium nibote microresonator," Opt. Lett. **44**, 1214–1217 (2019).
16. J. M. Ward and S. N. Chormaic, "Thermo-optical tuning of whispering gallery modes in Er:Yb co-doped phosphate glass microspheres," Appl. Phys. B **100**, 847–850 (2010).

[17]Y. Liu, L. Shi, X. Xu, P. Zhao, Z. Wang, S. Pu, and X. Zhang, "All-optical tuning of a magnetic-fluid-filled optofluidic ring resonator," Lab Chip **14**, 3004–3010 (2014).
[18]L. Xu, X. Jiang, G. Zhao, D. Ma, H. Tao, Z. Liu, F. G. Omenetto, and L. Yang, "High-Q silk fibroin whispering gallery microresonator," Opt. Express **24**, 20825–20830 (2016).
[19]L. Shi, T. Zhu, D. Huang, and M. Liu, "Thermo-optic tuning of integrated polymethyl methacrylate sphere whispering gallery mode resonator," IEEE Photonics J. **8**, 2701307 (2016).
[20]B. S. Lee, M. Zhang, F. A. S. Barbosa, S. A. Miller, A. Mohanty, R. St-Gelais, and M. Lipson, "On-chip thermo-optic tuning of suspended microresonators," Opt. Express **25**, 12109–12120 (2017).
[21]T. Lu, H. Lee, T. Chen, S. Herchak, J.-H. Kim, S. E. Fraser, R. C. Flagan, and K. J. Vahala, "High sensitivity nanoparticle detection using optical microcavities," Proc. Natl. Acad. U. S. A. **108**, 5976–5979 (2011).
[22]E. Kim, M. R. Foreman, M. D. Baaske, and F. Vollmer, "Thermal characterisation of (bio)polymers with a temperature-stabilised whispering gallery mode microsensor," Appl. Phys. Lett. **106**, 161101 (2015).
[23]S. Forstner, S. Prams, J. Knittel, E. D. van Ooijen, J. D. Swaim, G. I. Harris, A. Szorkovszky, W. P. Bowen, and H. Rubinsztein-Dunlop, "Cavity optomechanical magnetometer," Phys. Rev. Lett. **108**, 120801 (2012).
[24]S. Forstner, E. Sheridan, J. Knittel, C. L. Humphreys, G. A. Brawley, H. Rubinsztein-Dunlop, and W. P. Bowen, "Ultrasensitive optomechanical magnetometry," Adv. Mater. **26**, 6348–6353 (2014).
[25]W. Lin, H. Zhang, B. Liu, B. Song, Y. Li, C. Yang, and Y. Liu, "Laser-tuned whispering gallery modes in a solid-core microstructured optical fibre integrated with magnetic fluids," Sci. Rep. **5**, 17791 (2015).
[26]A. Mahmood, V. Kavungal, S. S. Ahmed, P. Kopcansky, V. Zavisova, G. Farrell, and Y. Semenova, "Magnetic field sensing using whispering-gallery modes in a cylindrical microresonator infiltrated with ferronematic liquid crystal," Opt. Express **25**, 12195–12202 (2017).
[27]J. A. Haigh, S. Langenfeld, N. J. Lambert, J. J. Baumberg, A. J. Ramsay, A. Nunnenkamp, and A. J. Ferguson, "Magneto-optical coupling in whispering-gallery-mode resonators," Phys. Rev. A **92**, 063845 (2015).
[28]A. Osada, R. Hisatomi, A. Noguchi, Y. Tabuchi, R. Yamazaki, K. Usami, M. Sadgrove, R. Yalla, M. Nomura, and Y. Nakamura, "Cavity optomagnonics with spin-orbit coupled photons," Phys. Rev. Lett. **116**, 223601 (2016).
[29]X. Zhang, N. Zhu, C.-L. Zou, and H. X. Tang, "Optomagnonic whispering gallery microresonators," Phys. Rev. Lett. **117**, 123605 (2016).
[30]J. F. Dillon, J. P. Remeika, and C. R. Staton, "Linear magnetic birefringence in cubic magnetic crystals," J. Appl. Phys. **40**, 1510–1511 (1969).
[31]S. Lan and M. Hossein-Zadeh, "Faraday effect in high-Q whispering-gallery mode optical cavities," IEEE Photonics J. **3**, 872–880 (2011).
[32]D. Sofikitis, L. Bougas, G. E. Katsoprinakis, A. K. Spiliotis, B. Loppinet, and T. P. Rakitzis, "Evanescent-wave and ambient chiral sensing by signal-reversing cavity ringdown polarimetry," Nature **514**, 76–79 (2014).
[33]M. L. Povinelli, S. G. Johnson, M. Loncar, M. Ibanescu, E. J. Smythe, F. Capasso, and J. D. Joannopoulos, "High-Q enhancement of attractive and repulsive optical forces between coupled whispering-gallery-mode resonators," Opt. Express **13**, 8286–8295 (2005).
[34]S. Vandendriessche, S. Van Cleuvenbergen, P. Willot, G. Hennrich, M. Srebro, V. K. Valev, G. Koeckelberghs, K. Clays, J. Autschbach, and T. Verbiest, "Giant Faraday rotation in mesogenic organic molecules," Chem. Mater. **25**, 1139–1143 (2013).
[35]C. T. Rodgers and P. J. Hore, "Chemical magnetoreception in birds: The radical pair mechanism," Proc. Natl. Acad. U. S. A. **106**, 353–360 (2009).